Structure of the $^6Li \rightarrow p+(n\alpha)$ vertex: $^6Li(e,e'p)n\alpha$ reaction

C. T. Christou,* D. R. Lehman, and W. C. Parke
Department of Physics, The George Washington University, Washington, D.C. 20052
(Received 8 September 1987)

Three-body models of ^6Li are used to describe the reaction $^6Li(e,e'p)n\alpha$. Under the impulse approximation, the differential cross section for the $^6Li(e,e'p)n\alpha$ reaction with unpolarized particles factorizes into a product of a kinematical factor, the (off-shell) electron-proton cross section, and a distorted spectral function of the ejected proton in the ^6Li nucleus. A prescription by de Forest is used to carry the ep cross section off the proton mass shell. The spectral function, containing all of the nuclear physics in the reaction, is found from the $^6Li \rightarrow p+(n\alpha)$ vertex amplitude. A unified theoretical description of both the bound state and the $(n\alpha)$ scattering state is employed to predict the $^6Li \rightarrow p+(n\alpha)$ vertex amplitude. For $(n\alpha)$ relative energies below 16 MeV and proton momenta below 200 MeV/c, the $P_{3/2}$ αN resonance dominates the shape of the spectral function. However, the contribution of the outgoing scattering wave due to the $S_{1/2}$ αN interaction has a significant role for momenta of the $(n\alpha)$ pair below 40 MeV/c, making the $2s$ orbitals in ^6Li control the behavior of the momentum distribution near zero momentum transfer to the $(n\alpha)$ pair. Recent coincidence experiments give good agreement with theory. Experimental resolutions are currently not quite capable of discriminating between various $S_{1/2}$ αN interactions used in the three-body calculation.

I. INTRODUCTION

Three-body models of the ^6Li nucleus have enjoyed remarkable success in describing both bound-state properties and scattering processes with energy transfers to the ^6Li nucleus less than that needed to excite the alpha particle, i.e., less than 20 MeV (see Ref. 3 for references). For ^6Li breakup reactions, the three-body model permits two-body and three-body breakup channels, with pairwise final-state interactions in each channel. The breakup of ^6Li into an alpha particle and a deuteron by electron scattering has recently been measured in the coincidence reaction $^6Li(e,e'd)\alpha$, and favorably compared to our calculation.[1,2] The theory successfully describes the $^6Li \rightarrow \alpha+d$ vertex for $\alpha-d$ relative momenta up to 300 MeV/c. The cross section can be related to the momentum distribution of the alpha-deuteron system in ^6Li. Sensitivity to both the detailed nature of the αN interaction and the tensor component of the NN interaction is evident.

Data from experiments involving the three-body breakup vertex, such as $^6Li(p,2p)n\alpha$, are available, but have been limited either by low incident projectile energy (making the impulse approximation dubious) or limited energy resolution. The $^6Li(e,e'p)n\alpha$ experiment has recently been used to map the valence proton momentum distribution in ^6Li with significant improvement in resolution over previous data. The experimental situation should improve even more dramatically in the near future, with new high-resolution $^6Li(e,e'p)n\alpha$ data at incident electron energies up to 800 MeV.

The electron scattering data will be unencumbered by strong interaction distortion effects due to initial and final state proton rescattering which complicate the $^6Li(p,2p)n\alpha$ cross-section calculation for low incident proton energies. With proper reaction kinematics, the analysis of the electron coincidence experiment allows for a clean separation of the momentum distribution of the bound proton and residual $(n\alpha)$ system from the electron-proton scattering event. Of course, the disadvantage of four orders of magnitude reduction in cross section makes the electron experiment correspondingly more difficult than with protons. The high-duty-factor electron facility at Southeastern Universities Research Association (SURA) promises to remedy the situation.

In anticipation of recent and proposed experiments on $^6Li(e,e'p)n\alpha$, we have applied our calculation of the $^6Li \rightarrow p+(n\alpha)$ vertex amplitude to $^6Li(e,e'p)n\alpha$. The derivation of the $^6Li \rightarrow p+(n\alpha)$ vertex amplitude was presented in Ref. 3. Reference 4 covers applications to the (p,2p) experiments. The present paper gives our results for the spectral function, momentum distribution, and cross section for electrons scattering from ^6Li in coincidence with a knocked-out proton.

Coincidence cross sections for the quasielastic reaction $^6Li(e,e'p)n\alpha$ have been measured over the past decade and a half. However, until a National Instituut voor Kernfysica en Hoge-Energiefysica (NIKHEF) experiment in Amsterdam[2] begun in 1985, results have had poor energy resolution and often inappropriate kinematics to make a discriminating comparison with three-body calculations for the reaction possible. Past data permits only crude tests of three-body models of ^6Li, and the input αN interactions.

In 1972, Antoufiev *et al.*[5] reported on an investigation of the reaction at incident energy of 1.2 GeV, with proton momentum transfer of 400 MeV/c and missing energy from -15 to $+30$ MeV. The experiment was limited to an energy resolution of 9 MeV. Hiramatsu *et al.*[6] obtained separation energy spectra and momentum dis-

tributions for an incident electron energy of 700 MeV. Kinematical constraints prevent extraction of low proton momentum transfer information. The data also were constrained by a 7 MeV energy resolution. Measurements were made by Heimlich *et al.*[7] at the Deutsches Elektronen-Synchrotron (DESY) in Hamburg in 1974, with incident electron energies of 2.5 and 2.7 GeV. The data were used to extract the proton momentum distribution in ^{6}Li in the range of 100–300 MeV/c. As before, the kinematics used made data for low proton momenta inaccessible. Beam energy resolution was near 12 MeV. In 1978, Nakamura *et al.*[8] measured the proton spectral function of ^{6}Li from (e,e'p) reactions at 700 MeV. They report both recoil momentum distributions for proton separation energies in five bins covering a range from threshold to 52 MeV, and proton separation energy spectra for recoil momenta in three bins from 20 to 200 MeV/c. Their separation energy resolution was near 7 MeV, with large experimental uncertainties for recoil momenta below $\sim$50 MeV/c.

The ^{6}Li(e,e'p)nα experiment was performed most recently at the NIKHEF-K electron accelerator in Amsterdam,[9] with an incident beam energy of 480 MeV and resolution of 0.25 MeV. Although higher beam energies would be more desirable to minimize proton (nα) rescattering effects, these data promise to have sufficient resolution to begin to discriminate among various models of the αN interaction used in a three-body calculation.

With incident electron energies significantly above 400 MeV, theoretical analyses of electron scattering (e,e'p) coincidence reactions often begin with the impulse approximation, permitting a factorization of the electron-proton differential cross section from the full coincidence cross section.[10] For ^{6}Li(e,e'p)nα, the remaining factors include a kinematical term and the distorted proton spectral function which depends on the momentum of the ejected proton in the original nucleus and the relative (nα) momentum.

To predict the spectral function, Nakamura *et al.*[11] used an independent-particle shell model with a Woods-Saxon potential in the development of a uniform picture of their (e,e'p) experiments at 700 MeV. Final state proton rescattering effects were estimated using a simplified phenomenological optical potential. They observe that the shell-model momentum distribution for the valence proton in ^{6}Li disagrees with the data.

A completely different and far more ambitious approach is taken by Strobel,[12] who begins with a six-body Schrödinger equation for the ^{6}Li nucleus. He separates off the center-of-mass motion and transforms to hyperspherical coordinates with a radial distance measured by the root of the sum of the distances of each nucleon from the center-of-mass squared. Yukawa type nucleonic potentials with a soft core are used for the pairwise interactions. To make the problem tractable, a truncation is performed, dropping terms with hyperangular quantum number above its minimum value. The truncation is justified by appeal to a hyperangular momentum barrier in the potential. The proton spectral energy function which follows[13] predicts the separation energy spectrum for tightly bound (1s) protons in ^{6}Li. There is fair agreement with experiment. No attempt was made to calculate the valence proton spectrum. Even with such a calculation, a consistent picture would require the application of the formalism to the p+(nα) scattering state. Hyperangular momentum quantum-number truncation would no longer be justified as it would in the bound state problem.

In this paper, we wish to present the results of applying our three-body model of ^{6}Li and a proper handling of the p+(nα) scattering state to the prediction of the spectral function for ^{6}Li$\rightarrow$p+(nα) in the ^{6}Li(e,e'p)nα cross section. Comparison with recent high resolution experiments promises to give a detailed test of the range and limitations of the model, and in particular to illuminate the behavior of the (nα) two-body interaction in the three-body system.

This paper is organized as follows: Sec. II describes the ^{6}Li(e,e'p)nα cross-section derivation, and discusses the conditions which allow the cross section for electrons on protons to be factorized from the full cross section. Included also is a discussion of how the electron-proton scattering structure functions are taken off shell. Section III presents our results for the nuclear spectral function and how its behavior can be interpreted physically. We give the consequent momentum distribution for valence protons in ^{6}Li and compare a set of models with available data. Section IV summarizes and gives our conclusions.

II. CROSS-SECTION DERIVATION

The cross section for ^{6}Li(e,e'p)nα takes an especially simple form if the kinematics of the reaction are arranged to permit proton-pole dominance, as in the reaction diagram of Fig. 1. For this type of reaction, the electron is assumed to have interacted with only one nucleon, which is subsequently detected. In a calculation, this assumption is the impulse approximation. Experimentally, the ejected nucleon must be given sufficient energy relative to the residual nucleus that rescattering effects can be neglected. From analysis of ^{6}Li(p,2p) experiments,[4,14] there is some evidence that proton distor-

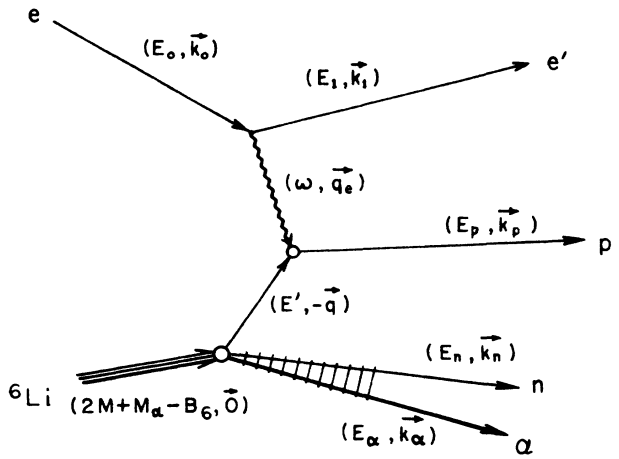

FIG. 1. Reaction diagram for the ^{6}Li(e,e'p)nα amplitude.

tion effects can be neglected when comparing theory to experiment for outgoing proton energies above 300 MeV.

During the reaction, the (nα) system recoils with momentum $\mathbf{q}=\mathbf{k}_\alpha+\mathbf{k}_n$, while $\kappa=(\mathbf{k}_\alpha-4\mathbf{k}_n)/5$ gives the relative momentum of the pair. The relative energy E_κ of the pair is then $5\kappa^2/8M$, where M is the nucleon mass (taken as 938 MeV). From the amplitude for the reaction, the differential cross section becomes

$$d\sigma=\tfrac{1}{6}\int\frac{1}{v_{\rm rel}}\sum_{m',s}|\mathcal{M}(m_0,m_1,m_p,m_n,m_6)|^2\,\delta(E_0-B_6-E_1-E_p-E_n-E_\alpha)$$
$$\times(2\pi)^4\delta^3(\mathbf{k}_0-\mathbf{k}_1-\mathbf{k}_p-\mathbf{q})d^3k_1d^3k_pd^3k_nd^3k_\alpha/(2\pi)^{12}\ . \tag{1}$$

With the factor $\frac{1}{6}$, the summation averages the initial spins and sums over final spins appropriate to unpolarized beams and targets. The quantity B_6 is the three-body binding energy of the ground state of ^{6}Li (near 4 MeV). In the laboratory frame, $v_{\rm rel}$ becomes p_0/E_0 for the incoming electron. Also, $d^3k_nd^3k_\alpha=d^3qd^3\kappa$.

Under the assumption of proton-pole dominance, the scattering amplitude $\mathcal{M}$ may be written in terms of the ep elastic scattering amplitude $M_{\rm ep}$ and the ^{6}Li three-body breakup vertex amplitude M as

$$\mathcal{M}(m_0,m_1,m_p,m_n,m_6)=\sum_{m_{p'}}\frac{M_{\rm ep}(m_0,m_p,m_1,m_{p'})M(\mathbf{q},\kappa;m_{p'},m_n,m_6)}{(E'+i\epsilon-q^2/2M)}\ . \tag{2}$$

In turn, the ^{6}Li three-body breakup amplitude M can be determined using the transition amplitude from the ^{6}Li ground state to a proton plane wave $|-\mathbf{q};m_{p'}\rangle$ and a (nα) scattering state $|\varphi_\kappa^{(-)}\rangle$:

$$M(\mathbf{q},\kappa;m_{p'},m_n,m_6)=\langle-\mathbf{q},\varphi_\kappa^{(-)};m_{p'},m_n|(V_{p\alpha}+V_{pn})|\Psi;m_6\rangle$$
$$=-(B_6+q^2/2\mu_{p,n\alpha}+\kappa^2/2\mu_{n\alpha})\langle-\mathbf{q},\varphi_\kappa^{(-)};m_{p'},m_n|\Psi;m_6\rangle\ . \tag{3}$$

The last step follows from application of the three-body Schrödinger equation for the (pnα) system. The reduced mass $\mu_{p,n\alpha}=5M/6$, while $\mu_{n\alpha}=4M/5$. Since the intermediate proton propagator matches the first factor in (3), the full amplitude for the reaction simplifies to:

$$\mathcal{M}(m_0,m_1,m_p,m_n,m_6)=\sum_{m_{p'}}M_{\rm ep}(m_0,m_p,m_1,m_{p'})A(\mathbf{q},\kappa;m_{p'},m_n,m_6)\ , \tag{4}$$

where

$$A(\mathbf{q},\kappa;m_{p'},m_n,m_6)=\int d^3p\,d^3k\,[\Phi_{-q}(\mathbf{p})\chi_{m_p}\varphi_\kappa^{(-)}(\mathbf{k})\chi_{m_n}]^\dagger\Psi_{m_6}(\mathbf{p},\mathbf{k})\ . \tag{5}$$

The calculation of the ^{6}Li→p+(nα) overlap amplitude $A(\mathbf{q},\kappa;m_{p'},m_n,m_6)$ was the subject of Ref. 3. There we observed that when the (nα) pair goes unobserved as in the ^{6}Li(e,e'p)nα experiment, the magnitude squared of the overlap amplitude can be integrated over the direction κ and averaged over the direction of $\mathbf{q}$. After summing over the polarization of the target and the outgoing neutron (m_6 and m_n), the remaining dependence on the proton magnetic quantum numbers becomes a Kronecker delta. Thus, for the full cross section, the double sum of $\mathcal{M}^\dagger\mathcal{M}$ over $m_{p'}$ in each $\mathcal{M}$ contracts to a single sum over $M_{\rm ep}^\dagger M_{\rm ep}$, making it possible to factorize the ep elastic cross section from the full differential cross section for ^{6}Li(e,e'p)nα. Physically, this means that if the target and recoil particle polarizations are unobserved, and if the orientation of the relative momentum for the recoiling pair is unmeasured, then the ejected proton cannot communicate any polarization to the scattered electron.

The ^{6}Li(e,e'p)nα cross section (1) now becomes:

$$\frac{d^4\sigma}{d\Omega_1d\Omega_pdE_1dE_\kappa}=\left[\frac{k_pE_p}{|1-E_p\mathbf{k}_p\cdot\mathbf{q}/E_q(k_p)^2|}\right]\times\left[\frac{d\sigma}{d\Omega_{\rm ep}}\right]_{\rm w.r.f.}[\mu_{n\alpha}\kappa V(\kappa,q)]\ , \tag{6}$$

where the term in large square brackets contains kinematical factors, the term in large parenthesis holds the ep elastic cross section without a recoil factor (w.r.f.) and with the proton off its mass-energy shell, while the last factor, the spectral function $S(E_\kappa,q)$, contains the nuclear part of the ^{6}Li(e,e'p)nα cross section:

$$S(E_\kappa,q)=\mu_{n\alpha}\kappa V(\kappa,q)\ , \tag{7}$$

with

$$V(\kappa,q)=\tfrac{1}{3}\sum_{m_n,m_{p'},m_6}\int d\Omega_qd\Omega_\kappa|A(\mathbf{q},\kappa;m_{p'},m_n,m_6)|^2/4\pi\ . \tag{8}$$

Because of the completeness of the outgoing scattering states, the joint momentum distribution $V(\kappa,q)$ satisfies a sum rule:

$$4\pi \int q^2 dq \int \kappa^2 d\kappa V(\kappa,q)=1 , \tag{9a}$$

or, in terms of the spectral function:

$$4\pi \int q^2 dq \int dE_\kappa S(E_\kappa,q)=1 . \tag{9b}$$

(If any one of the three protons in ^{6}Li could have been knocked out, then this sum would have been 3.)

The ep elastic scattering recoil factor,

$$[1/|1+(2E_0/M)\sin^2(\theta/2)|] ,$$

is not contained in the ep cross section in Eq. (6), since now it is the residual p+(nα) system which takes up the momentum transferred by the electron, contributing to the kinematical factor above. Since the exchanged proton is off its mass-energy shell, the free proton Rosenbluth cross section may not be a good approximation for the free-electron bound-proton elastic scattering cross section. Bincer[15] has used relativistic invariance arguments to show that the most general half-off-shell ep vertex function can be written in terms of three form factors. In the on-shell limit, only two independent form factors survive. Thus, on-shell electron-nucleon scattering does not contain enough information to determine all three form factors. Barring a good theoretical model, extrapolating the on-shell ep scattering amplitudes to half-off-shell ones will lead to ambiguities. de Forest[16] compared a variety of extrapolation recipes. Starting with a general form for the ep cross section satisfying Lorentz and gauge invariance:

$$\left[\frac{d\sigma}{d\Omega_{ep}}\right]_{\text{w.r.f.}} = \sigma_M \left\{ \frac{q_e^4}{\mathbf{q}_e^4} w_C + \left[\frac{q_e^2}{2\mathbf{q}_e^2} + \tan^2(\theta/2) \right] w_T + \frac{q_e^2}{\mathbf{q}_e^2} \left[\frac{q_e^2}{\mathbf{q}_e^2} + \tan^2(\theta/2) \right]^{1/2} \cos\varphi \; w_I + \left[\frac{q_e^2}{\mathbf{q}_e^2} \cos^2\varphi + \tan^2(\theta/2) \right] w_S \right\} , \tag{10}$$

he imposed the constraints of nucleonic current conservation and a finite limit for the cross-section as the electron four momentum q_e^2 approaches zero (photon point) to specify the nucleonic structure functions w above. In the cross-section expression, $\mathbf{q}_e^2$ is the electron three-momentum transfer squared, φ is the angle between the scattering plane and the plane defined by the vectors $\mathbf{k}_p$ and $\mathbf{q}_e$, as in Fig. 2. The factor σ_M is the Mott cross section:

$$\sigma_M = \frac{\alpha^2 \cos^2(\theta/2)}{4E_0^2 \sin^4(\theta/2)} . \tag{11}$$

The four nucleonic structure functions are given by

$$\begin{aligned} w_C &= (\tfrac{1}{4}E_q E_p)\{(E_q+E_p)^2[F_1^2+(q_e^2/4M^2)\kappa_a^2 F_2^2] \\ &\quad -\mathbf{q}_e^2(F_1+\kappa_a F_2)^2\} , \\ w_T &= (q_e^2/2E_q E_p)(F_1+\kappa_a F_2)^2 , \\ w_S &= (k_p^2 \sin^2\gamma/E_q E_p)[F_1^2+(q_e^2/4M^2)\kappa_a^2 F_2^2] , \\ w_I &= -(k_p \sin\gamma/E_q E_p)(E_q+E_p)[F_1^2+(q_e^2/4M^2)\kappa_a^2 F_2^2] . \end{aligned} \tag{12}$$

The angle γ is formed between $\mathbf{k}_p$ and the electron momentum transfer $\mathbf{q}_e$. The energy of the virtual photon ω found in $q_e^2=\omega^2-\mathbf{q}_e^2$ is fixed by assuming that the intermediate proton is on its mass-energy shell, so that $\omega=E_p-E_q$, where $E_q=(\mathbf{q}^2+M^2)^{1/2}$. $F_1(q_e^2)$ and $F_2(q_e^2)$ are the Dirac and Pauli form factors for the proton, with κ_a the anomalous magnetic moment of the proton.

III. RESULTS AND DISCUSSION

The nuclear physics of the ^{6}Li(e,e'p)nα reaction is contained in the spectral function $S(E_\kappa,q)$ of Eq. (7). This in turn is determined by the joint momentum distribution $V(\kappa,q)$, which gives the probability density of finding a proton moving with momentum of magnitude q relative to the center of mass of an interacting (nα) pair which have a relative momentum magnitude κ. As described in Ref. 3, $V(\kappa,q)$ has a prominent peak for E_κ from 0.7 to 0.8 MeV and q near 0.35 fm^{-1} due to the resonant $P_{3/2}$(nα) pair interaction, with a background contribution from rescattering in the $S_{1/2}$ and $P_{1/2}$ (nα) partial waves. The relatively large value for $V(\kappa,q)$ for $q=0$ is caused by the overlap of the S wave part of the plane and (nα) rescattering waves in the outgoing three-body system with a 2s proton in the ^{6}Li ground state. Although the effect of the S-wave overlap is not as prominent in the spectral function as it is in the joint momentum distribution, $S(E_\kappa,q)$ will also show a nonzero value as q approaches zero, except at $E_\kappa=0$. Our calculated spectral function is shown in Fig. 3 for the three-body model which takes an attractive-projected

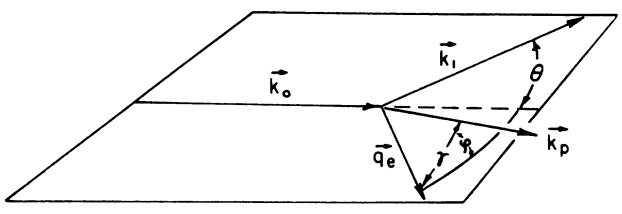

FIG. 2. Momenta geometry for the ^{6}Li(e,e'p)nα reaction.

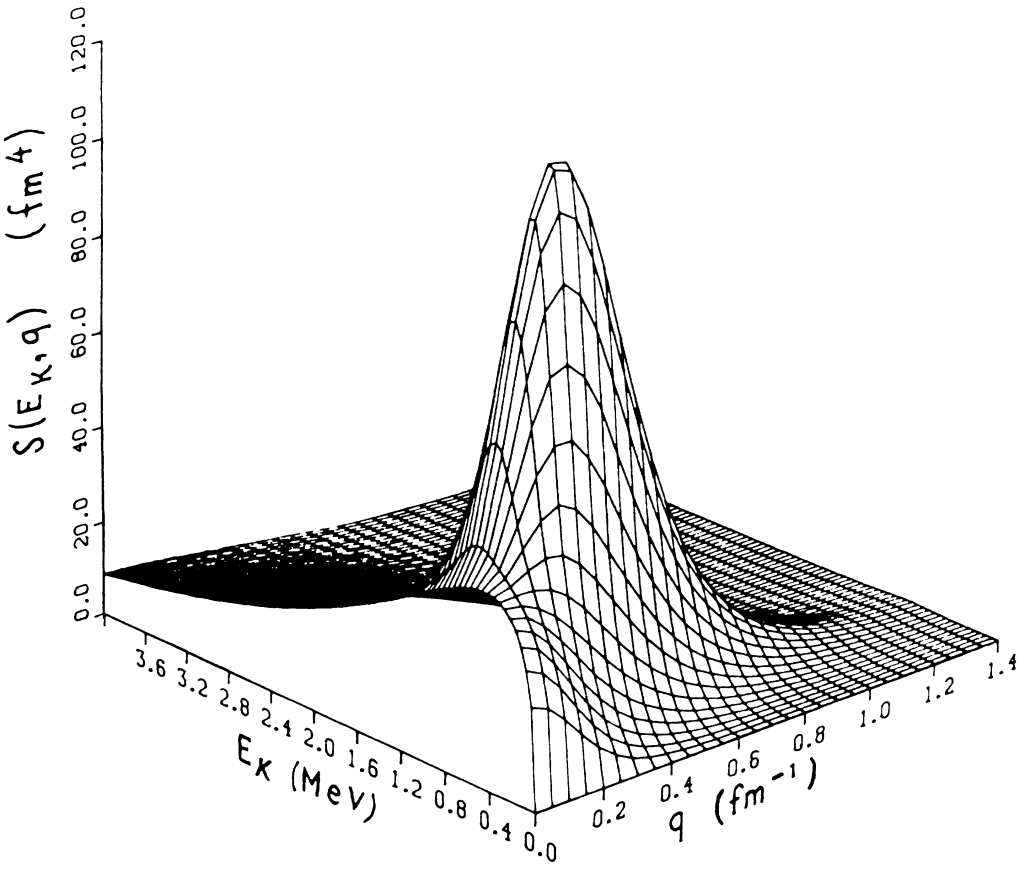

FIG. 3. ^{6}Li→p+(nα) spectral function; attractive-projected $S_{1/2}$ (nα) interaction.

$S_{1/2}$ αN interaction and a tensor component of the NN interaction which gives 4% D state in the deuteron wave function. We should emphasize that once the two-body interactions are characterized and made to agree with known two-body scattering data, there are no free parameters in the calculation, nor are any truncations made in the three-body equations which determine both the ground state ^{6}Li and scattering state p+(nα) wave functions. In Fig. 4, we show the difference between the spectral functions of the attractive-projected $S_{1/2}$ αN interaction model and the repulsive $S_{1/2}$ αN interaction model. Model sensitivity is generally weak, but evident at low q and around the $P_{3/2}$ αN resonance peak.

For experiments which measure the coincidence cross section:

$$\frac{d^3\sigma}{d\Omega_1 d\Omega_p dE_1} = \int_{E_{\kappa_{\min}}}^{E_{\kappa_{\max}}} (\mathrm{kf}) \left[\frac{d\sigma}{d\Omega_{ep}}\right]_{\mathrm{w.r.f.}} \mu_{n\alpha}\kappa V(\kappa,q) dE_\kappa \ , \tag{13}$$

i.e., for those which do not measure the energy of the outgoing proton, the data may still be used to extract the proton momentum distribution:

$$\rho(q) = \int_{E_{\kappa_{\min}}}^{E_{\kappa_{\max}}} V(\kappa,q)\kappa^2 d\kappa = \int_{E_{\kappa_{\min}}}^{E_{\kappa_{\max}}} S(E_\kappa,q) dE_\kappa \ , \tag{14}$$

provided the kinematical factor and the ep cross section can be approximated by a constant over the kinematical range of E_κ. This is often a good approximation, since both the kinematical factor and the ep cross section are relatively smooth for q below 200 MeV/c, within the kinematical range of E_κ.

For example, consider the fixed electron kinematics in the proposed experiment of Mougey and Frullani,[17] for which $E_0=550$ MeV, $\theta=62°$, $q_e=550$ MeV/c, $\omega=155$ MeV. The kinematical factor is near 0.124×10^{-2} fm^{-4}, while $(d\sigma/d\Omega)_{ep}=0.624\times10^{-5}$ fm^2 in the range $0<E_\kappa<3.0$ MeV and for $q=0.7$ fm^{-1}. Near $q=0$, the integration range of E_κ becomes zero, resulting in no cross section in this region. The allowed range of E_κ broadens with increasing q, becoming $0\le E_\kappa\le 116$ MeV for $q=1.4$ fm^{-1}. Figure 5 shows the threefold coincidence cross-section for these kinematics. The nucleon form factors F_1 and F_2 used in the ep cross section are those of Höhler *et al.*[18] The solid curve shows the prediction of the attractive-projected $S_{1/2}$ αN interaction model, while the dash line gives that of the repulsive $S_{1/2}$ αN interaction model.

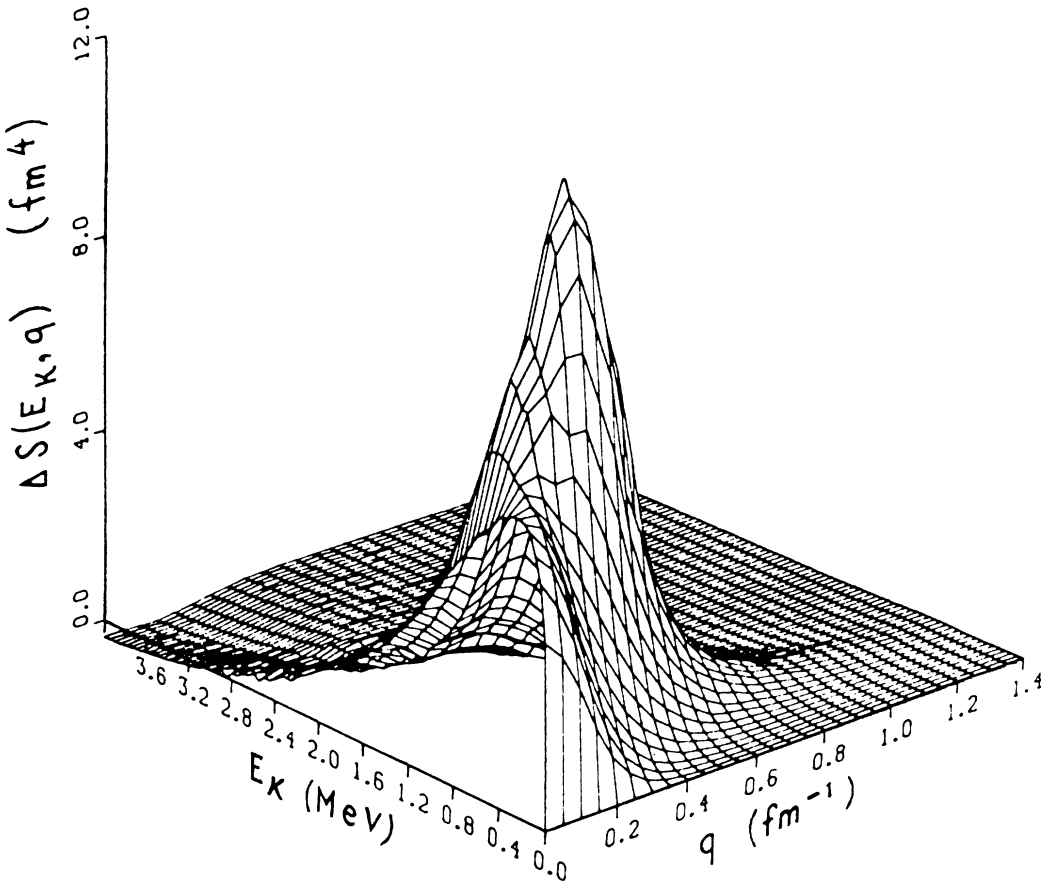

FIG. 4. ^{6}Li→p+(nα) spectral function difference; attractive-projected minus repulsive $S_{1/2}$ (nα) interaction models.

For the purposes of exploring the nature of the αN interaction, fixed electron kinematics prevent a full mapping of the nuclear spectral function. Values of the cross section for q near zero will necessarily be small because of the restricted phase space (the range of E_κ is proportional to q for small q). Moreover, this restriction for low but allowed values of q excludes the $P_{3/2}$ αN resonant peak from contributing. Clearly, the unbounded nature of the (nα) system requires a kinematical analysis based on a true three-body final state. Although the position of the $P_{3/2}$ αN resonance in the spectral function $S(E_\kappa,q)$ is essentially at the energy value E_κ found in free nucleon-alpha particle scattering, its position in q is determined by the full three-body dynamics of the ^{6}Li ground state together with the p+(nα) scattering state. Dramatic effects of the $S_{1/2}$ αN interaction are found at low q.

In contrast to fixed electron kinematics, if the two measured scattering angles for the electron and proton are held fixed while measuring the outgoing electron and proton energies, then the nuclear spectral function can be fully examined. This variable electron kinematics experiment is similar in arrangement to that of (p,2p) experiments discussed in Ref. 4.

The ^{6}Li→p+(nα) momentum distribution, $\rho(q)$, is shown in Fig. 6 after integrating $S(E_\kappa,q)$ over the $P_{3/2}$ peak with E_κ ranging from 0 to 2.0 MeV. The nonzero value of $\rho(q)$ at $q=0$ is directly accountable by a finite probability for a 2s valence proton in the ground state of ^{6}Li which overlaps with the S wave parts of p+(nα) outgoing scattered wave in the final state. The peaks take their strength from the $P_{3/2}$ αN interaction. The

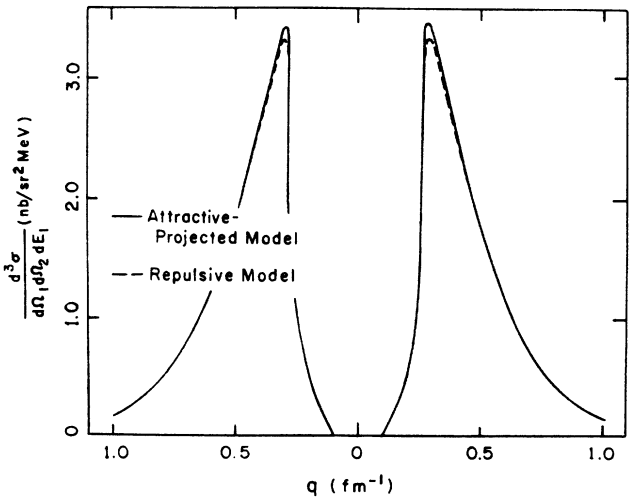

FIG. 5. Coincidence cross section for ^{6}Li(e,e'p)nα; fixed electron kinematics.

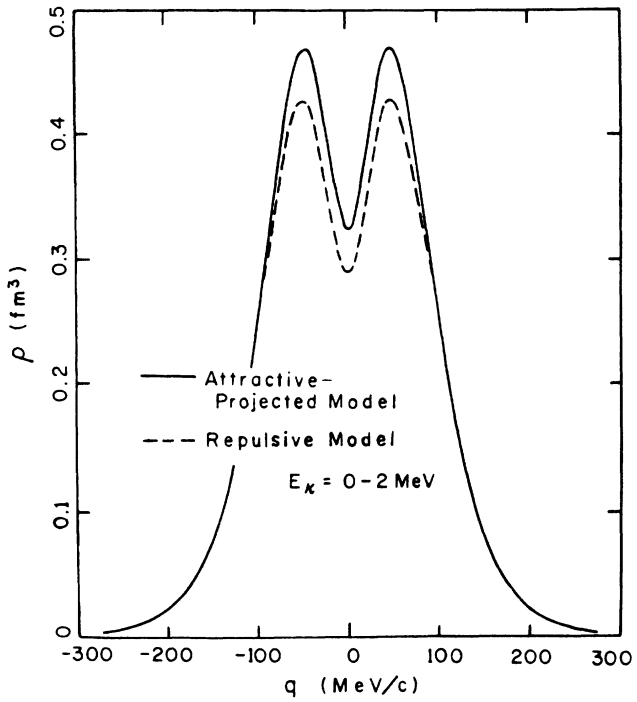

FIG. 6. ^{6}Li→p+(nα) momentum distribution; repulsive vs attractive-projected $S_{1/2}$ (nα) interaction, E_κ=0–2.0 MeV.

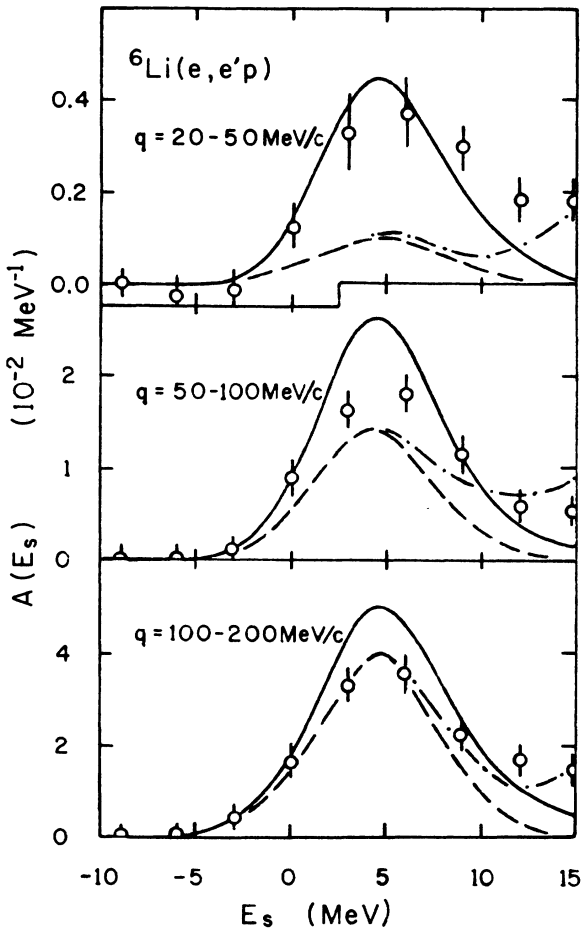

FIG. 7. Proton separation energy spectra for ^{6}Li(e,e'p)nα. Solid curves come from our repulsive $S_{1/2}$ αN interaction model. Data and the nonsolid shell-model curves come from Ref. 8. The shell-model dashed-dot curve includes 1s proton knockout.

figure suggests that with sufficient resolution, the detailed behavior of the αN interaction may be explored, going beyond what can be known from two body scattering data. The attractive projected $S_{1/2}$ αN interaction model has an attractive potential together with an added projective term to exclude any spurious (nα) bound state. The result is a representation of the interaction between a nucleon and a composite nuclear system (the alpha particle) which contains an implicit representation of the Pauli principle. The repulsive $S_{1/2}$ αN interaction, which naturally avoids the Pauli principle, agrees with the $S_{1/2}$ αN phase shifts just as well as the attractive-projected model in the range of energies tested by our three-body model.

In Figs. 7–9 we show a comparison of our calculation with the data from Nakamura *et al.* Because of the large width of the energy uncertainty in E_κ, we first integrated $S(E_\kappa,q)$ over a normalized Gaussian with a full width at half maximum of 6.8 MeV. The resolution-folded spectra can then be averaged over the reported energy bands in the separation energy $E_s=E_\kappa+B_6$ which cover the $P_{3/2}$ αN resonance peak (E_s below 7 MeV) and the background below the alpha particle breakup threshold (E_s from 7 to 16 MeV) resulting in the recoil momentum distributions. We can also compare with the reported proton separation-energy spectra by integrating $S(E_\kappa,q)$ over particular ranges of q:

$$A(E_\kappa)=4\pi\int_{q_1}^{q_2} q^2 dq\bar{S}(E_\kappa,q)\ . \tag{15}$$

The results are shown in Fig. 7 for q in the ranges of 20–50, 50–100, and 100–200 MeV/c. The separation energy spectra for the 20–50 MeV/c range is dominated by the effects of the $S_{1/2}$ αN interaction. The 50–100 and 100–200 MeV/c plots cover the $P_{3/2}$ αN resonance peak in the spectral function. The theory comes from the repulsive $S_{1/2}$ αN interaction model, which fixes not only the behavior of the spectra, but also its absolute normalization. In Figs. 8 and 9, the recoil momentum distributions are shown. The figures clearly show the inadequacy of the shell model calculation. However, this experiment did not have sufficient energy resolution nor accuracy at low q to serve as a test of our models.

Preliminary indications suggest that the new data from NIKHEF on the ^{6}Li(e,e'p)nα experiment agree well with our calculation.

IV. SUMMARY AND CONCLUSIONS

This paper is third in a series of three papers on the three-body ^{6}Li→p+(nα) vertex and applies our results for the vertex amplitude to the prediction of the nuclear spectral function in the ^{6}Li(e,e'p)nα reaction cross sec-

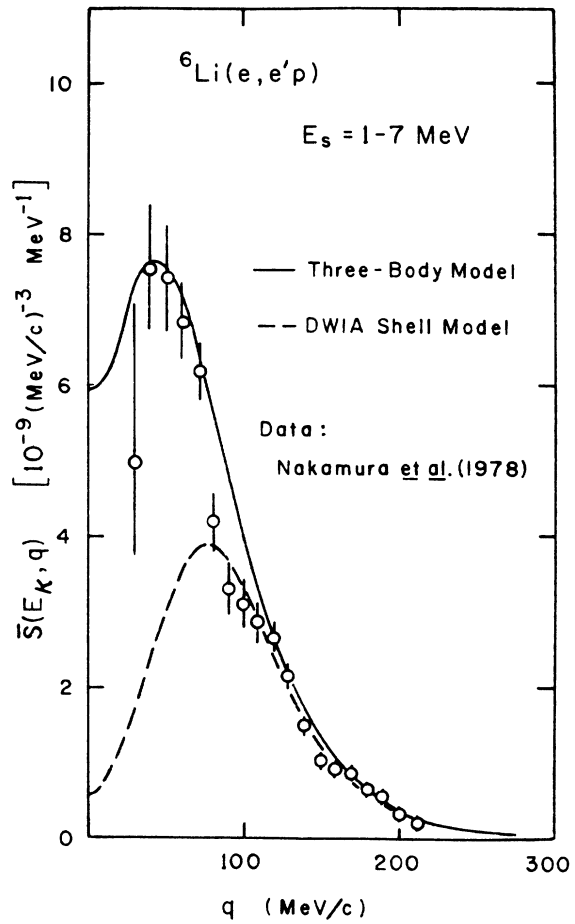

FIG. 8. Recoil momentum distribution for $E_s = 1-7$ MeV. The solid curve comes from our repulsive $S_{1/2}$ αN interaction model. Data and the dashed shell-model curve come from Ref. 8.

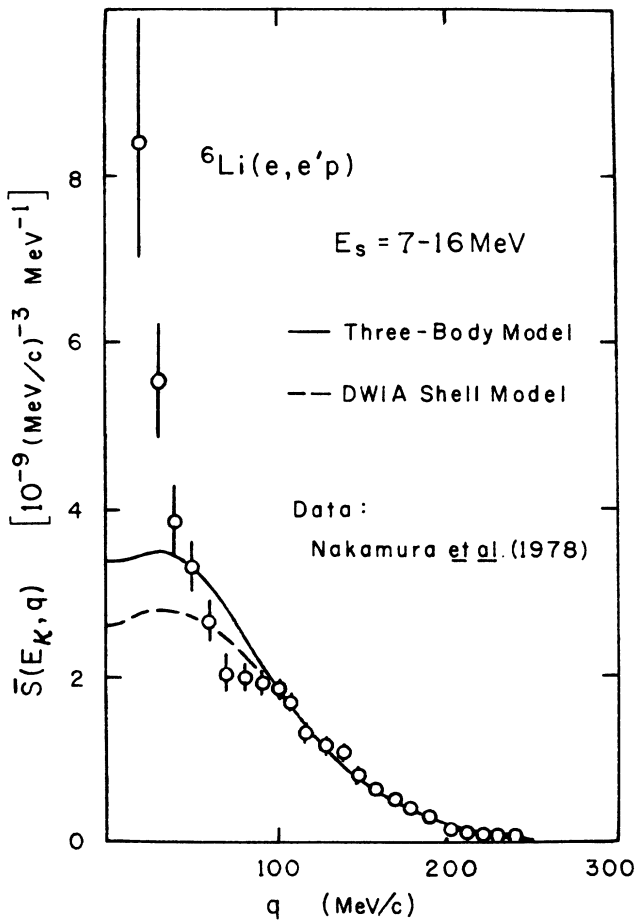

FIG. 9. Recoil momentum distribution for $E_s = 7-16$ MeV. The solid curve comes from our repulsive $S_{1/2}$ αN interaction model. Data and the dashed shell-model curve come from Ref. 8.

tion. Data currently available for this reaction do not have sufficient resolution or accuracy to discriminate among different models of the input two-body interactions in the three-body calculation. With new high duty-factor electron accelerators, electron coincidence experiments show great promise in unveiling the detailed nature of the two-body forces in nuclei. In particular, the behavior of the nucleon-alpha particle interaction both on- and off-the-mass shell can be investigated unencumbered by rescattering of the projectile particles. We have shown that different models for the $S_{1/2}$ αN interaction which match experimental two-body phase shifts can have measurably different effects in the three-body system. Having a good understanding of this interaction will have wide application for few body calculations in nuclear physics. New electron coincidence experiments with variable electron kinematics promise to resolve the remaining ambiguity.

This work has been supported in part by the U.S. Department of Energy under Grant No. DE-FG05-86-ER40270.

*Present address: Naval Research Laboratory, Code 4651 Washington, D.C. 20375.

[1]C. T. Christou, C. J. Seftor, W. J. Briscoe, W. C. Parke, and D. R. Lehman, Phys. Rev. C **31**, 250 (1985).

[2]R. Ent, H. P. Blok, J. F. A. Van Hienen, G. Van der Steenhoven, J. F. J. van den Brand, J. W. A. den Herder, E. Jans, P. H. M. Keizer, L. Lapikas, E. N. M. Quint, P. K. A. de Witt Huberts, B. L. Berman, W. J. Briscoe, C. T. Christou, D. R. Lehman, B. E. Norum, and A. Saha, Phys. Rev. Lett. **57**, 2367 (1986).

[3]C. T. Christou, D. R. Lehman, and W. C. Parke, Phys. Rev. C **37**, 445 (1988).

[4]C. T. Christou, D. R. Lehman, and W. C. Parke, Phys. Rev. C **37**, 458 (1988).

[5]Y. P. Antoufiev, V. L. Agranovich, V. S. Kuzmenko, and P. V. Sorokin, Phys. Lett. **B42**, 347 (1972).

[6]H. Hiramatsu, T. Kamae, H. Muramatsu, K. Nakamura, N. Izutsu, and Y. Watase, Phys. Lett. **B44**, 50 (1973).
[7]F. H. Heimlich, F. Rossle, M. Kobberling, J. Moritz, K. H. Schmidt, D. Wegener, D. Zeller, J. K. Bienlem, J. Bleckwenn, and H. Dinter, Nucl. Phys. **A228**, 478 (1974).
[8]K. Nakamura, S. Hiramatsu, T. Kamae, and H. Muramatsu, Nucl. Phys. **A296**, 431 (1978).
[9]P. K. A. deWitt Huberts, private communication.
[10]U. Amaldi, Jr., Supl. Nuovo Cimento **5**, 1225 (1967).
[11]K. Nakamura, S. Hiramatsu, T. Kamae, and H. Muramatsu, Nucl. Phys. **A268**, 381 (1976).
[12]G. L. Strobel, Phys. Rev. C **18**, 2395 (1978).
[13]G. L. Strobel, Phys. Rev. C **20**, 364 (1979).
[14]F. Prats, Nucl. Phys. **A227**, 469 (1974).
[15]A. M. Bincer, Phys. Rev. **118**, 855 (1960).
[16]T. De Forest, Jr., Nucl. Phys. **A392**, 232 (1983).
[17]J. Mougey and S. Frullani, private communication.
[18]G. Höhler, E. Pietarinen, I. Sabb-Stefanescu, F. Borkowski, G. G. Simon, V. H. Walther, and R. D. Wendling, Nucl. Phys. **B114**, 505 (1976).